# Dual-Specificity Tyrosine Phosphorylation-Regulated Kinase 1A Does Not Require Tyrosine Phosphorylation for Activity in Vitro†

Tatyana Adayev, Mo-Chou Chen-Hwang, Noriko Murakami, Eric Lee, David C. Bolton, and Yu-Wen Hwang*

*Molecular Biology Department, New York State Institute for Basic Research in Developmental Disabilities, Staten Island, New York 10314*

*Received February 6, 2007; Revised Manuscript Received April 14, 2007*

ABSTRACT: The dual-specificity tyrosine phosphorylation-regulated kinase 1A (*DYRK1A*) gene is localized in human chromosome 21, and its overexpression has been associated with the learning and memory deficits of Down syndrome. DYRK1A contains a $Y^{319}XY^{321}$ motif shared by all members of the DYRK protein kinase family. Residue Y321 in the motif is phosphorylated in DYRK1A prepared from *Escherichia coli* and from eukaryotic cells. It has been proposed that the YXY motif is an equivalent of the TXY motif, the activation loop, of mitogen-activated protein kinase and that phosphorylation at the motif is required for DYRK activity. In this study, the role of tyrosine phosphorylation in the activity of DYRK1A was investigated in detail. Wild-type DYRK1A with a reduced level of phosphotyrosine (pY) was prepared by treating *E. coli*-produced DYRK1A with two different protein tyrosine phosphatases. The resulting pY-depleted DYRK1A could not regain pY during autophosphorylation but was as active as the untreated control. These findings were further supported by the observation that DYRK1A retained significant enzymatic activity when both tyrosine residues in the YXY motif were replaced with either histidine or glutamine. Together, we conclude that tyrosine phosphorylation and tyrosine residues in the YXY motif are not directly involved in DYRK1A enzymatic activity in vitro.

DYRK1A (*1*) is the mammalian ortholog of *Drosophila* minibrain kinase (MNB) (*2*). Both DYRK1A and MNB belong to the DYRK protein kinase family (*3*), which includes yeast Yak1p (*4*), several related DYRKs (*5*−*7*), and many others (*8*−*11*). The human *DYRK1A* gene is mapped to the q22.2 section of chromosome 21, termed the Down syndrome critical region (*12*−*14*). Several lines of evidence have implicated this gene in Down syndrome (*15*, *16*).

In addition to the conserved kinase subdomains common to all kinases (*17*), members of the DYRK family contain several characteristic sequence features unique to this family (*3*). One of them, the YXY motif, is found between kinase subdomains VII and VIII (*3*). DYRK1A is distantly related to mitogen-activated protein kinase (MAPK)[1] (*18*). Molecular modeling based on the crystal structures of extracellular regulated kinase 2 (ERK2), a member of the MAPK family, has suggested that the $Y^{319}XY^{321}$ motif of DYRK1A is equivalent to the ERK2's TXY motif, the activation loop (*18*, *19*). Phosphorylation of both threonine and tyrosine in the TXY motif by upstream kinases activates ERK2 (*20*). Despite the name of dual specificity, DYRK1A has so far been shown to function only as a proline/arginine-directed serine/threonine kinase toward exogenous substrates (*21*−*30*).

Recombinant DYRK1A produced in *Escherichia coli* and in mammalian cells is enzymatically active and contains phosphotyrosine (pY) at Y321 in the YXY motif (*1*, *19*). The Y321F substitution produces a protein with a low pY content and a greatly reduced kinase activity (*1*, *19*). On the other hand, Y319 of the YXY motif is not phosphorylated and the Y319F mutant has activity similar to that of the wild-type protein (*1*, *19*). Therefore, it was hypothesized that phosphorylation, probably through autophosphorylation, at Y321 in the YXY motif is required for DYRK1A activity (*1*, *19*). Evidence obtained from other members of the DYRK family, *Saccharomyces cerevisiae* Yak1p (*31*), *Saccharomyces pombe* Pom1p (*11*), mammalian MIRK/DYRK1B (*6*), DYRK3 (*32*), and *Drosophila* DYRK2 (dDYRK2) (*33*), also appears to support the notion that the YXY motif phosphorylation is important for the catalytic activity of these kinases. In dDYRK2 and MNB, tyrosine autophosphorylation was found to occur only during protein synthesis but not in the mature protein (*34*). Thus, tyrosine autophosphorylation was proposed to be a "one-off" inceptive event for kinase activation (*34*). In an initial attempt to prepare the "inactive" DYRK1A, *E. coli*-produced wild-type (WT) DYRK1A was treated with leukocyte antigen-related (LAR) protein tyrosine phosphatase. LAR readily removes pY from DYRK1A.

† This work is supported in part by New York State Office of Mental Retardation and Developmental Disabilities and by NIH Grants HD38295 (Y.-W.H.) and HD43960 (to Dr. Jerzy Wegiel).

* To whom correspondence should be addressed: Molecular Biology Department, New York State Institute for Basic Research in Developmental Disabilities, 1050 Forest Hill Rd., Staten Island, NY 10314. Telephone: (718) 494-5337. Fax: (718) 494-5905. E-mail: hwang@mail.csi.cuny.edu.

[1] Abbreviations: D3, dynatide 3; FF, DYRK1A (Y319F/Y321F) mutant; HH, DYRK1A (Y319H/Y321H) mutant; QQ, DYRK1A (Y319Q/Y321Q) mutant; ERK2, extracellular regulated kinase; GST, glutathione *S*-transferase; GST-497, truncated GST-DYRK1A containing residues 1−497; GST-FL, full-length GST-DYRK1A; LAR, leukocyte antigen-related protein tyrosine phosphatase; MAPK, mitogen-activated protein kinase; pS, phosphoserine; pT, phosphothreonine; pY, phosphotyrosine; pY-dep, pY-depleted; WT, wild type.

10.1021/bi700251n CCC: $37.00 
Published on Web 05/31/2007

However, to our surprise, DYRK1A lacking pY was as active as the untreated control. Therefore, the role of tyrosine phosphorylation on DYRK1A was investigated in detail. Our results indicate that neither tyrosine phosphorylation nor tyrosine residues in the YXY motif are absolutely required for the activity of DYRK1A in vitro.

## MATERIALS AND METHODS

*Clone Construction*. The GST fusion full-length (GST-FL) DYRK1A clone, the truncated (GST-497) DYRK1A clone, and human Gli 1 (*35*) expression vector (pcGli1) were described previously (*36*, *37*). Vector, pMNB, for expressing intact (nonfusion) DYRK1A was constructed by inserting the DYRK1A fragment from the GST fusion vector (*36*) into T7 RNA polymerase vector pND1 through the ClaI and XhoI sites as described previously (*38*). Construction of the FF mutant was described previously (*36*). HH and QQ mutants were prepared by site-directed mutagenesis using the following oligonucleotides, agttggggcagagaattcaccagcatattcagagtcgcttcta and agttggggcagagaattcaacagcagattcagagtcgcttcta, respectively, as the mutagenic primer. The mammalian vectors for expressing the full-length YXY motif mutant were first constructed as the pRHC-Mnb clone (*27*). The *DYRK1A* gene in the resulting pRHC-Mnb(mutant) clone was then spliced into the pcDNA3 vector (Invitrogen) through the HindIII and XhoI sites to produce pcMnb-(mutant) vectors as described previously (*36*, *37*).

*Protein Preparation*. All protein preparations were performed at 0−4 °C except where indicated otherwise. Full-length (either with or without GST fusion) DYRK1A was purified with Ni-NTA resin, while all GST-497 constructs were purified with glutathione resin as described previously (*36*, *39*). pY-dep DYRK1A was prepared as follows. Protein tyrosine phosphatase hydrolysis was performed by treating 10 $\mu$g of DYRK1A in a 100 $\mu$L reaction mixture with either 25 units of LAR (New England Biolabs) or 400 units of $\lambda$PPase (New England Biolabs) at 30 °C in each respective buffer (supplied by the manufacturer) for 40 min. The "untreated" DYRK1A was prepared in parallel as described above but without phosphatase. If necessary, both untreated and pY-dep DYRK1A were repurified from reaction mixtures by using glutathione resin. The resin-bound DYRK1A was washed three times with the washing buffer [25 mM Tris-HCl (pH 7.4), 100 mM NaCl, and 0.1% Triton X-100] and then eluted with 10 mM glutathione in 0.1 M Tris-HCl (pH 7.4). Glutathione in the eluted samples was subsequently reduced by repetitive washing and concentration with the Triton-free washing buffer in a Millipore Microcon YM-10 filter. Samples were then stored at −70 °C until they were used. The effectiveness of phosphatase treatment was monitored by immunoblotting using anti-pY antibodies.

*Antibodies and Immunological Assays*. Both anti-pY antibodies, PY-99 and PY-20, were purchased from Santa Cruz Biotechnology. Mouse monoclonal anti-DYRK1A antibody 7F3 was produced as described previously (*40*). Antibody 7F3 was batch purified from the ascites fluid by using Bakerbond Abx (J. T. Baker). Immunoblotting was performed using chemiluminescent reagent CDP-Star as described previously (*36*).

*Kinase Assays*. pY regeneration (autophosphorylation) was performed in a 30 $\mu$L reaction mixture containing 1 $\mu$g of DYRK1A in a kinase buffer [25 mM HEPES (pH 7.4), 5 mM $MgCl_2$, and 100 mM NaCl] as previously described (*1*, *36*). The reactions were initiated by the addition of 10−500 $\mu$M ATP (final concentration) and were allowed to proceed at 30 °C. At the indicated times, a 5 $\mu$L aliquot was withdrawn, boiled in SDS−PAGE protein loading buffer, and used for immunoblotting analysis. When necessary, autophosphorylation was performed in the presence of 2 $\mu$Ci of [$\gamma$-$^{32}$P]ATP (specific activity of 2.66 Ci/mmol). Incorporation of phosphate into DYRK1A was assessed by precipitating a 5 $\mu$L aliquot of reaction mixture together with 100 $\mu$g of BSA in 2 mL of 4% silicotungstic acid in 3 N sulfuric acid, collected onto a glass fiber filter (Whatman GF/C), and quantified in a scintillation counter. DYRK1A activity was measured in a 30 $\mu$L reaction mixture containing kinase buffer, 100 ng of DYRK1A, 1 $\mu$g of substrate (see below), and 2 $\mu$Ci of [$\gamma$-$^{32}$P]ATP (specific activity of 2.66 Ci/mmol). The reaction was initiated by the addition of kinase. When dynamin 1 was used as the substrate, incorporation of phosphate was assessed in a 5 $\mu$L timed-withdrawn aliquot by the acid precipitation protocol as described above. When D3 peptide was used as the substrate, incorporation of phosphate was assessed via a phosphocellulose (Whatman P81) membrane binding assay (*27*). Kinetic parameters for truncated WT, HH, and QQ were determined as previously described (*37*).

*Phospho-Amino Acid Analysis.* Phospho-amino acid analysis was performed according to the method of Hunter and Sefton (*41*) as described previously (*27*).

*Gli 1-Dependent Transcription Assay*. Gli 1-dependent transcription was conducted on COS7 cells exactly as described previously (*37*).

*MS Analysis of Phosphorylated Peptides.* Control and pY-dep WT GST-497 samples were further purified by SDS−PAGE for MS analysis. The PAGE step was necessary for removal of Brij 35 used in the LAR reaction buffer. The GST-497 band was sliced from the PAGE gel after a brief staining with Coomassie Blue. The protein was then destained, reduced, modified with iodoacetamide, and digested in gel with trypsin essentially as described previously (*42*). The digested peptides were then prepurified with an OMIX micro extraction tip (Varian, Inc.) as suggested by the manufacturer. The solution recovered was dried and reconstituted in 25 $\mu$L of solvent A (0.1% formic acid in water), and portions were loaded on a Symmetry C18 nanoAcquity column (180 $\mu$m × 20 mm) as two or three sequential 4.1 $\mu$L injections for either MS-only runs (33% of the sample) or MS/MS runs (49% of the sample). Following the last injection, the peptides were resolved on an Atlantic dC18 nanoAcquity column (100 $\mu$m × 100 mm) using one of two different complex gradients of solvent B (0.1% formic acid in acetonitrile) using a nanoAcquity UPLC system (Waters). The percentage of solvent B in the first gradient increased from 5% (flow rate of 0.6 $\mu$L/min) to 18% at 10 min (flow rate of 0.4 $\mu$L/min) to 30% at 90 min, 40% at 100 min, 70% at 105 min, and 90% at 109 min (all at a flow rate of 0.4 $\mu$L/min). The percentage of solvent B in the second gradient increased from 0% (flow rate of 0.6 $\mu$L/min) to 15% at 15 min (flow rate of 0.4 $\mu$L/min) to 20% at 25 min (flow rate of 0.25 $\mu$L/min), 35% at 85 min, 40% at 95 min, 50% at 105 min, 60% at 110 min, and 90% at 115 min (all at a flow rate of 0.25 $\mu$L/min). The eluent from the column was

analyzed directly on a Q-TOF Micro mass spectrometer (Waters Corp.) equipped with a nanoflow electrosprayer and scanned for *m*/*z* 200 to 1990 at 1.1 s intervals. An external lock mass standard (leucine enkephalin, *m*/*z* 556.2771) was analyzed through a separate orthogonal electrosprayer at 22 or 30 s intervals, depending on the exact method that was being used. The data were collected in either MS mode for quantifying phosphorylated peptides or the survey mode for determination of structures by fragmentation and MS/MS analysis. The quantification of peptides was performed using MassLynx 4.0 as briefly described here. Chromatograms were created from each data set by plotting a 1Da window around the *m*/*z* values of interest. The chromatographic peaks were confirmed to have the component of interest by summing the mass spectra across the peak and determining the centroid *m*/*z* values, followed by deconvolution and transformation to the accurate mass value of the one plus ion. The ion envelope encompassing mass isomers containing zero to three $^{13}C$ atoms (obtained prior to TOF transformation) was plotted to create the chromatogram of the specific peptide. Both the phosphorylated and nonphosphorylated forms of the IYQYIQSR peptide eluted as single peaks, with the phosphorylated form having a slightly shorter retention time. Estimates of the relative amount of each peptide were determined by two different methods. The first relied on the integrated peak areas obtained using the integration function in MassLynx, and the second used the peak height of the one plus ion from the peak obtained from the TOF transformation routine. Both methods yielded essentially the same results. The amount of phosphorylated IYQYIQSR peptide was determined relative to the amount of nonphosphorylated IYQYIQSR peptide in the same sample (pY/pY-dep). The percentage reduction in the amount of phosphorylated IYQYIQSR peptide after phosphatase treatment was determined by the formula $100 \times (pY_{control}/pY\text{-}dep_{control} - pY_{treated}/pY\text{-}dep_{treated})/(pY_{control}/pY\text{-}dep_{control})$.

## RESULTS

*Dephosphorylation of E. coli-Expressed DYRK1A by LAR Protein Tyrosine Phosphatase.* GST fusion DYRK1A containing the first 497 residues of the kinase, GST-497 (*37*), was selected for the initial study. GST-497 includes the entire kinase domain (residues 160−480) of DYRK1A and an additional 160 residues to its N-terminal end. The construct, expressed as an 85 kDa polypeptide (see Figure 8), retains a catalytic activity similar to that of the full-length protein (*37*).

Like full-length WT DYRK1A (*1*, *19*), *E. coli*-expressed WT GST-497 was recognized by the anti-pY antibodies PY-99 (Figure 1A,B). Upon LAR hydrolysis, pY in GST-497 was quickly removed and reached a level below the limit of detection by antibody PY-99 (Figure 1A,B). LAR treatment did not alter the levels of total GST-497 protein, which was evident in immunoblots employing anti-DYRK1A antibody 7F3 (*40*) (Figure 1C). The removal of pY from WT GST-497 by LAR hydrolysis was further confirmed by a second anti-pY antibody PY-20 (Figure 1D) as well as mass spectrometry (Table 2). However, PY-20 was less sensitive than PY-99 in detecting WT GST-497. Therefore, antibody PY-99 was used for subsequent experiments unless noted otherwise. The ability to prepare WT GST-497 depleted of pY, designated pY-dep, permitted us to examine the role of tyrosine phosphorylation in DYRK1A activity by using the WT protein directly.

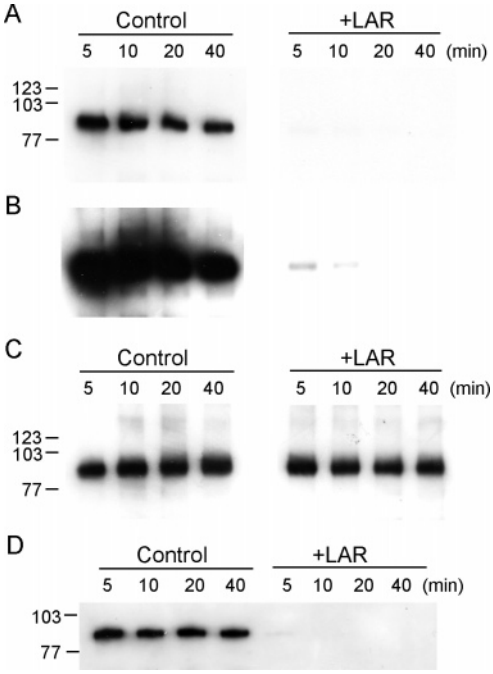


FIGURE 1: Dephosphorylation of WT GST-497 by LAR. LAR hydrolysis was performed in a 100 $\mu$L reaction mixture containing 10 $\mu$g of *E. coli*-expressed WT GST-497 as described in Materials and Methods. The reaction was initiated by the addition of LAR. At the indicated times, aliquots of the reaction mixture were withdrawn and subjected to immunoblotting against antibodies PY-99 (A and B), 7F3 (C), and PY-20 (D). Controls were samples similarly prepared without the addition of LAR. The amount of GST-497 used for immunoblotting was 20 ng for antibody 7F3 and 100 ng for antibodies PY-99 and PY-20. Panels B was the same as panel A except that it was overexposed.

*Activity of LAR-Treated WT GST-497.* LAR-treated pY-dep and untreated WT GST-497 were prepared and repurified using glutathione resin. These proteins were first assessed for their ability to regain pY through autophosphorylation under the conditions normally used to measure DYRK1A activity (*1*, *36*). The incubation did not lead to pY production in pY-dep WT GST-497 for at least 20 min at 30 °C (Figure 2A). However, a very low level of pY could be detected after incubation for 40−80 min (Figure 2B). The incubation did not alter the pY level in untreated DYRK1A (Figure 2A,B), nor did it change the level of total protein (Figure 2C). Probing with antibody PY-20 also supported the conclusion that little or no pY was regenerated after autophosphorylation (Figure 2D).

Although pY-dep WT GST-497 was repurified after LAR treatment, the level of residual LAR remaining in the preparation was not known. To rule out the possibility that the failure to regain pY may be due to contaminating LAR, autophosphorylation was performed in the presence of phosphatase inhibitor sodium vanadate ($Na_3VO_4$). $Na_3VO_4$ at 1 mM completely inhibited LAR (Figure 3A), while it marginally affected the activity of DYRK1A, as measured by the phosphorylation of dynatide 3 (D3) (Figure 3B), a peptide substrate derived from the major DYRK1A phosphorylation site of dynamin 1xa (*27*). As shown in Figure 3C, pY-dep WT GST-497 did not regain pY even in the presence of $Na_3VO_4$. This finding indicates that the inability to regain pY in pY-dep WT GST-497 is unlikely to be due

Table 1: MS/MS Fragmentation of YXY Peptides from Control WT GST-497

| precursor mass $[M + 2H]^{2+}$ | ion series | calculated mass (error) I | Y | Q | Y | I | Q | S | R |
|---|---|---|---|---|---|---|---|---|---|
| 535.7852 | a | 86.097 (−0.005) | 249.160 (−0.001) | —[a] | —[a] | —[a] | —[a] | —[a] | —[a] |
| | b | —[a] | 277.155 (−0.004) | 405.214 (−0.001) | 568.277 (0.010) | 681.361 (0.022) | 809.420 (0.025) | 896.452 (0.012) | —[a] |
| | y | —[a] | 957.479 (0.017) | 794.416 (−0.004) | 666.357 (−0.005) | 503.294 (−0.003) | 390.210 (0.006) | 262.152 (−0.012) | 175.120 (−0.003) |
| | z | —[a] | —[a] | 777.389 (−0.020) | —[a] | —[a] | 373.184 (−0.015) | —[a] | —[a] |

| precursor mass $[M + 2H]^{2+}$ | ion series | calculated mass (error) I | Y | Q | pY | I | Q | S | R |
|---|---|---|---|---|---|---|---|---|---|
| 575.7718 | a | 86.097 (−0.004) | 249.160 (−0.007) | —[a] | —[a] | —[a] | —[a] | —[a] | —[a] |
| | b | —[a] | 277.155 (−0.004) | 405.214 (−0.001) | 648.243 (0.005) | 761.327 (0.029) | 889.386 (−0.026) | 976.418 (0.035) | —[a] |
| | y | —[a] | 1037.446 (0.011) | 874.382 (0.004) | 746.324 (−0.001) | 503.294 (0.001) | 390.210 (−0.004) | 262.152 (−0.002) | 175.120 (0.000) |
| | z | —[a] | 1020.419 (0.042) | 857.356 (0.007) | 729.297 (−0.010) | —[a] | —[a] | —[a] | —[a] |

[a] No matching fragment ion.

Table 2: Reduction of pY321 by Phosphatase Hydrolysis

| | ratio of YXY peptides (phosphorylated/unphosphorylated) | | % of reduction (treated/control) | |
|---|---|---|---|---|
| treatment | trial 1 | trial 2 | trial 1 | trial 2 |
| control[a] | 9.70 | 2.46 | — | — |
| LAR | 2.15 | 1.30 | 77.8 | 47.2 |
| control[b] | 0.975 | 0.695 | — | — |
| λPPase | 0.029 | 0.015 | 97.0 | 97.8 |

[a] Incubated in LAR buffer. [b] Incubated in λPPase buffer.

to the contaminating LAR. The inability to regain pY in pY-dep WT GST-497 cannot be attributed to a limitation in DYRK1A and ATP concentration, as similar results were obtained with up to 33 μM DYRK1A (Figure S1) and 500 μM ATP (data not shown). This inability of pY-dep DYRK1A to regain pY is similar to that of dDYRK2 and MNB (*34*).

Interestingly, if autophosphorylation was conducted in the presence of [$\gamma$-$^{32}$P]ATP, both pY-dep and untreated WT GST-497 were found to incorporate [$^{32}$P]phosphate with a slow but an indistinguishable rate (Figure 4A). This result indicates that pY-dep WT GST-497 is as active as the untreated counterpart in catalyzing autophosphorylation. To identify the phosphorylated amino acid residues that resulted from autophosphorylation, pY-dep and untreated WT GST-497 were autophosphorylated in the presence of [$\gamma$-$^{32}$P]ATP for 30 min and subjected to phospho-amino acid analysis. The results in Figure 4B show that while phosphoserine (pS) and phosphothreonine (pT) were readily detectable in both pY-dep and untreated WT GST-497, pY was not detected in either sample. This finding is consistent with the result of anti-pY antibody staining (Figure 2A,B,D) and confirms that no pY was regenerated for at least the first 30 min of autophosphorylation.

Subsequently, the ability of pY-dep and untreated WT GST-497 to phosphorylate exogenous substrates was examined. The time course of phosphorylation shows that both

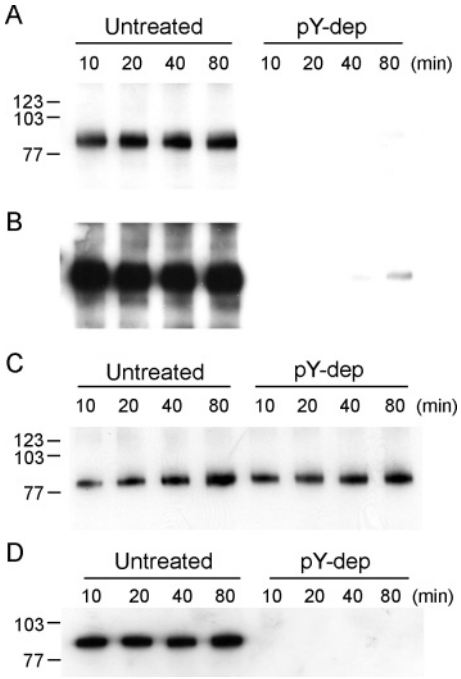


FIGURE 2: Autophosphorylation of pY-dep WT GST-497. pY-dep and untreated WT GST-497 were prepared and subjected to autophosphorylation as described in Materials and Methods in the presence of 50 μM ATP. At the indicated times, aliquots of the reaction mixture were withdrawn and subjected to immunoblotting against antibodies PY-99 (A and B), 7F3 (C), and PY-20 (D) as described in the legend of Figure 1. Panel B is panel A overexposed.

pY-dep and untreated WT GST-497 have a similar activity in phosphorylating D3 and dynamin 1 (Figure 5). In fact, no change in kinase activity of WT GST-497 was observed even when the reactions were performed either with LAR-treated WT GST-497 that was not repurified or with extra LAR added to the reaction mixture (data not shown). In summary, we conclude that LAR treatment does not affect DYRK1A activity.

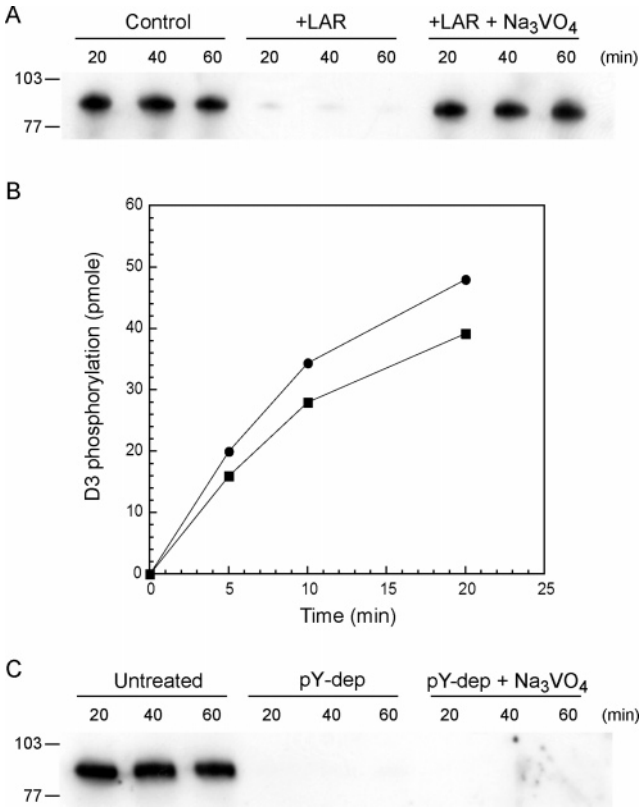


FIGURE 3: Effects of $Na_3VO_4$ on the activity of LAR and DYRK1A. (A) Inhibition of LAR by $Na_3VO_4$. LAR hydrolysis was performed similarly as described in the legend of Figure 1 except that 1 mM $Na_3VO_4$ was included in the assay. At the indicated times, aliquots of the reaction mixture were withdrawn and subjected to immunoblotting against antibody PY-99. Controls were samples without LAR and $Na_3VO_4$. (B) Measurement of DYRK1A activity in the presence of $Na_3VO_4$. DYRK1A activity was measured as the extent of $^{32}P$ incorporation into D3 in a 30 $\mu$L reaction mixture containing 1 $\mu$g of D3 and 100 ng of WT GST-497 with or without 1 mM $Na_3VO_4$ as described in Materials and Methods. Data were corrected for backgrounds (D3 alone and kinase alone samples) before they were plotted. The data represent the average of three independent trials: (●) without and (■) with $Na_3VO_4$. (C) Autophosphorylation of pY-dep WT GST-497 in the presence of $Na_3VO_4$. pY-dep (LAR) and untreated WT GST-497 samples were prepared and subjected to an autophosphorylation assay as described in the legend of Figure 2 with the addition of 1 mM $Na_3VO_4$. At the indicated times, aliquots of DYRK1A were withdrawn and probed with antibody PY-99.

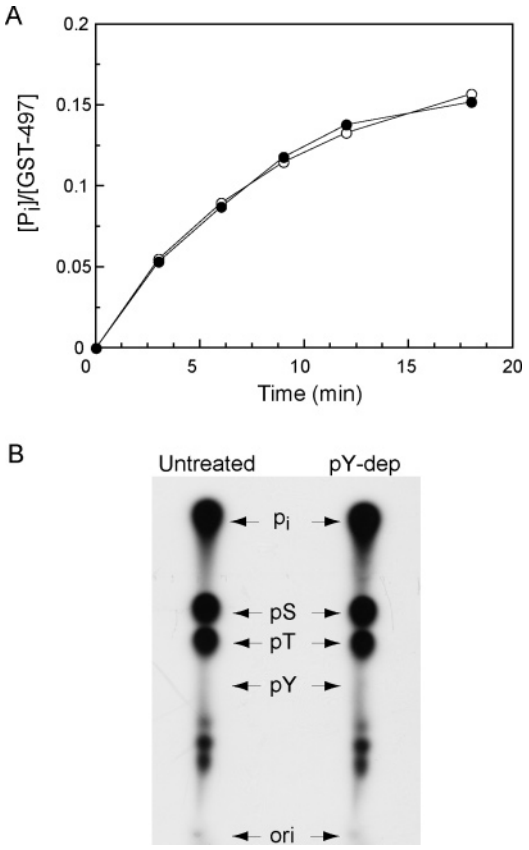


FIGURE 4: Autophosphorylation (A) and phospho-amino acid analysis (B) of pY-dep and untreated WT GST-497. (A) pY-dep (LAR) and untreated WT GST-497 were autophosphorylated in the presence of [$\gamma$-$^{32}P$]ATP as described in Materials and Methods. The stoichiometry of phosphate incorporation was determined from acid-precipitated $^{32}P$-labeled proteins. The data represent the average of three independent trials: (●) untreated WT GST-497 and (○) pY-dep (LAR) WT GST-497. (B) Phospho-amino acid profile. Autophosphorylated samples of untreated and pY-dep WT GST-497 from panel A were subjected to phospho-amino acid analysis as described previously (*27*). $P_i$ represents free phosphate, and ori represents origin.

*Dephosphorylation of WT GST-497 by λ Protein Phosphatase (λPPase).* λPPase was previously shown to remove pY and to reduce correspondingly the catalytic activity of dDYRK2 and MNB (*33*, *34*), two members of the DYRK family. Therefore, we examined the effects of λPPase hydrolysis on the activity of WT GST-497. Like LAR treatment, pY in WT GST-497 could be readily removed by λPPase and reached a level essentially below the level of detection by antibody PY-99 (Figure 6A; see also Table 2). This observation is in direct contrast with that of dDYRK2 and MNB as λPPase removed pY only partially from these two proteins (*33*, *34*). We then measured the activity of λPPase-treated WT GST-497 without further repurification. λPPase treatment caused an ~30−40% reduction in the "apparent" activity of WT GST-497 to phosphorylate D3 (Figure 6B). Unlike LAR, λPPase is a broad-spectrum protein phosphatase (*43*, *44*) and DYRK1A-phosphorylated D3 is a good substrate of this phosphatase (Figure S2). Therefore, we suspected that the apparent reduction in kinase activity was due to the presence of λPPase. Repurification of λPPase-treated WT GST-497 by glutathione resin did not improve the apparent activity in λPPase-treated WT GST-497 (data not shown). However, the addition of 1 mM $Na_3VO_4$ to the reaction mixture, a condition inhibiting λPPase hydrolysis of DYRK1A-phosphorylated D3 (Figure S2), fully restored the activity of λPPase-treated WT GST-497 to that of the untreated control (Figure 6B). This result indicates that the action of λPPase is the cause for the apparent activity reduction in λPPase-treated WT GST-497. As in LAR treatment, we conclude that λPPase dephosphorylation also does not affect DYRK1A activity.

*Dephosphorylation of pY321 by LAR and λPPase.* To verify dephosphorylation at pY321 by protein tyrosine phosphatase hydrolysis, we characterized the YXY motif containing tryptic peptide, $^{318}$IYQYIQSR, by mass spectrometry (MS). MS detected a pair of $[M + 2H]^{2+}$ ions with the mass and the charge envelope matching that of unphosphorylated (*m*/*z* 535.7856) and singly phosphorylated IYQYIQSR peptides (*m*/*z* 575.7688), respectively (Figure 7A). The identity of these ions was subsequently confirmed by MS/MS fragmentation. An example of MS/MS fragmen-

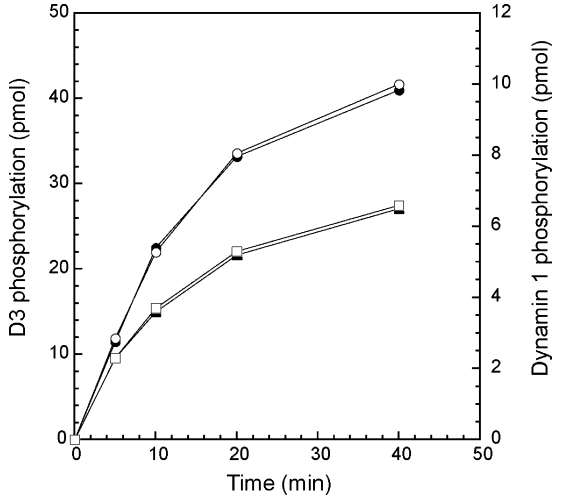


FIGURE 5: Catalytic activity of LAR-treated WT GST-497. LAR-treated pY-dep and untreated WT GST-497 were similarly prepared, repurified, and then subjected to activity measurement by using D3 [(●) untreated and (○) pY-dep on the left *y*-axis] or dynamin 1 [(■) untreated and (□) pY-dep on the right *y*-axis] as the substrate as described in the legend of Figure 3.

tation of the unphosphorylated YXY peptides and phosphorylated YXY peptides from control WT GST-497 is shown in Table 1. MS/MS fragmentation confirmed that Y321 was the phosphorylated residue, while no phosphorylation was detected at Y319 (Table 1). The levels of the two $[M + 2H]^{2+}$ ions were quantified as described in Materials and Methods. Although the level of phosphorylated peptides and unphosphorylated peptides cannot be directly compared due to a potential difference in ionization efficiency, the detection of a comparable level of both peptides, more the phosphorylated peptide than the unphosphorylated one in some cases (Table 2), suggests that Y321 is significantly phosphorylated in *E. coli*-expressed WT GST-497. If one assumes that the two peptides have the same ionization efficiency, the stoichiometry of Y321 phosphorylation would be at least ~40% (Table 2). The phosphorylated form but not the unphosphorylated form of the HINEVY$^{111}$YAK peptide was also detected (data not shown), suggesting that Y111 is fully phosphorylated in WT GST-497. Y111 phosphorylation was not detected in DYRK1A expressed in mammalian cells (*19*), and mutation at this residue did not alter the activity of DYRK1A (*19*). Y111 phosphorylation in *E. coli*-expressed WT GST-497 may only be a byproduct of DYRK1A activity. Nevertheless, the phosphorylation profile of WT GST-497 identified in our study is in accord with that of another *E. coli*-expressed DYRK1A truncated mutant (containing residues 1−498) determined previously by others (*19*).

Subsequently, we investigated the change in the levels of pY321 in GST-497 upon phosphatase treatment. Both LAR and λPPase could readily hydrolyze pY321 from WT GST-497, but the phosphorylated YXY peptide could still be detected (Figure 7B and Table 2). Therefore, we developed a scale using the relative ratio of the unphosphorylated to phosphorylated YXY peptide within the sample to evaluate the extent of dephosphorylation (Table 2). Clearly, pY321 in GST-497 was substantially reduced upon LAR or λPPase treatment, and λPPase appears to have removed nearly all pY321. On the other hand, no pY111-containing peptide was detected in either LAR- or λPPase-treated samples (data not

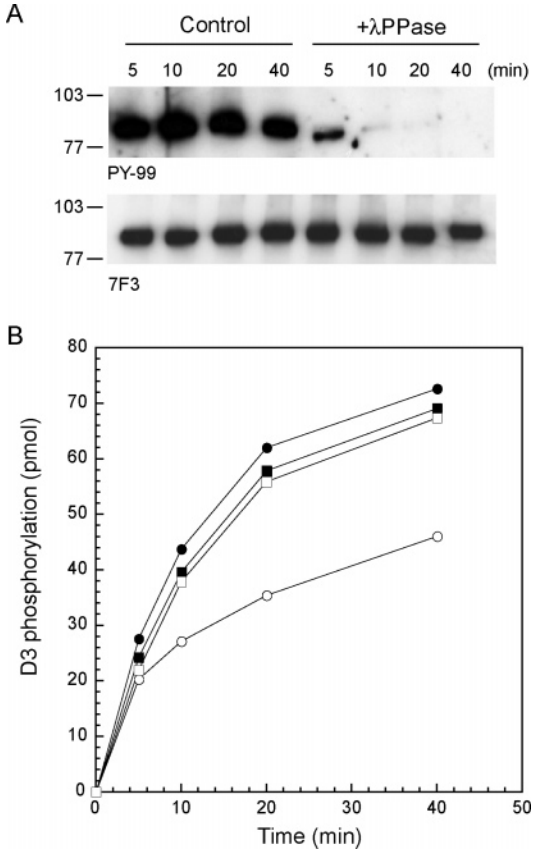


FIGURE 6: Dephosphorylation of WT GST-497 by λPPase treatment (A) and catalytic activity of λPPase-treated WT GST-497 (B). (A) λPPase hydrolysis was performed in a 100 μL reaction mixture containing 10 μg of *E. coli*-expressed WT GST-497 and 400 units of λPPase as described in Materials and Methods. At the indicated times, aliquots of the reaction mixture were withdrawn and subjected to immunoblotting against antibodies PY-99 and 7F3. Controls were samples similarly prepared without the addition of λPPase. The amount of GST-497 used for immunoblotting was 20 ng for antibody 7F3 and 100 ng for antibody PY-99. (B) λPPase-treated and untreated WT GST-497s were then used without repurification for phosphorylating D3: untreated WT GST-497 (●), λPPase-treated WT GST-497 (○), untreated WT GST-497 with 1 mM $Na_3VO_4$ (■), and λPPase-treated WT GST-497 with 1 mM $Na_3VO_4$ (□). All data represent the average of three independent trials.

shown). This result suggests that pY at Y111 is stoichiometrically hydrolyzed by either phosphatase.

*Kinetic Activity of pY-dep Full-Length WT DYRK1A.* To show that our findings are not an artifact of protein truncation, experiments were also performed with GST fusion full-length WT DYRK1A (GST-FL) expressed in *E. coli*. The GST-FL preparation consists of multiple pY-containing polypeptides ranging in size from 95 to 125 kDa (the predicated size of GST-FL) (Figure S3). Probing with a few different anti-DYRK1A antibodies recognizing different regions of DYRK1A suggests that all these polypetides were derived from the full-length protein, and the degradation appears to start from the C-terminal end of the polypeptide (data not shown).

Like the case in GST-497, pY in GST-FL was readily dephosphorylated by LAR as revealed by antibodies PY-99 and PY-20 (Figure S3). Thus, pY-dep WT GST-FL was prepared and subjected to autophosphorylation. Both antibodies, PY-99 and PY-20, failed to detect pY-dep WT GST-FL that has been autophosphorylated for up to 60 min (Figure

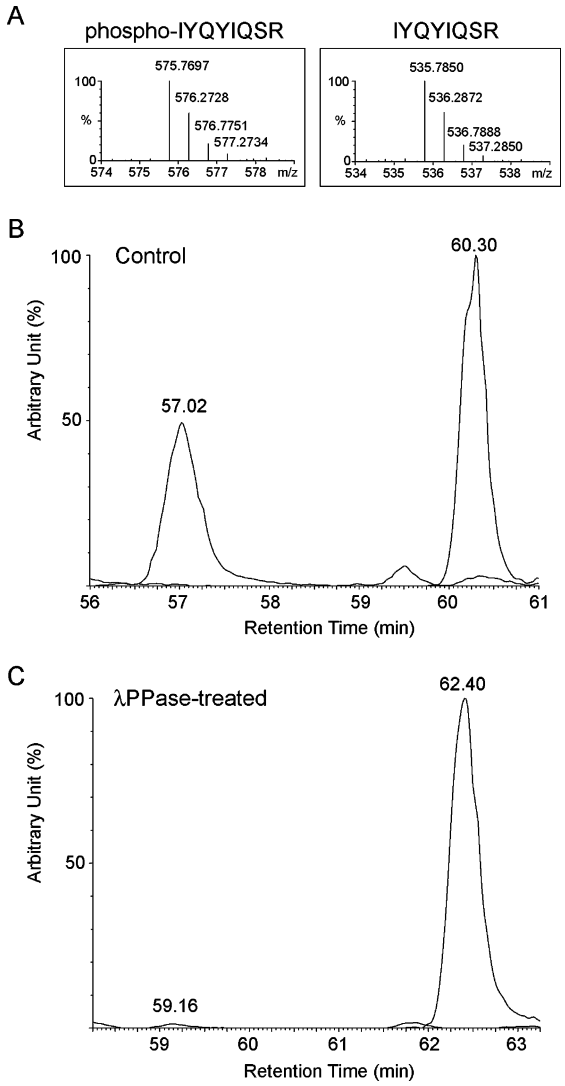


FIGURE 7: MS analysis of YXY peptides. DYRK1A was digested with trypsin and subjected to MS analysis. (A) Accurate mass ion profiles of the phosphorylated and unphosphorylated IYQYIQSR peptides show the characteristic ion envelopes obtained from the centroid accurate mass spectra for the $[M + 2H]^{2+}$ ions from the peaks shown in panel B (57.02 and 60.30 min, respectively). The identities of each peptide and the ion profiles were confirmed in separate MS/MS analyses. Chromatographic profiles of the phosphorylated and unphosphorylated forms of the IYQYIQSR peptide in control (B) and λPPase-treated (C) WT GST-497 were plotted from the liquid chromatography−mass spectrometry data as described in Materials and Methods. The chromatograms show only the MS ion counts for the $[M + 2H]^{2+}$ ions of the mass isomers containing zero to three $^{13}C$ atoms for phospho-IYQYIQSR (*m*/*z* 575.6−577.4) and IYQYIQSR (*m*/*z* 535.5−537.4). The ion intensities determined at 1.1 s intervals were summed and smoothed. The *y*-axis scales are 5100 (B) and 10 800 (C) ions per second full scale. Differences in column equilibration conditions caused the retention times for both peptides to shift somewhat between individual runs. However, the phospho-IYQYIQSR peptide emerged consistently ~3 min earlier than the unphosphorylated one from the reverse-phase column under the experimental conditions that were used. The peak area for each peptide was integrated and used to calculate the ratio of YXY peptides (Table 2). The minor peak eluting at approximately 59.5 min in the control sample does not contain the IYQYIQSR peptide.

S3). Despite lacking pY, pY-dep WT GST-FL had an activity identical to that of the untreated control in phosphorylating D3 (Figure S4) and intact dynamin 1 (data not shown). These results indicate that the mode of action of WT GST-FL is

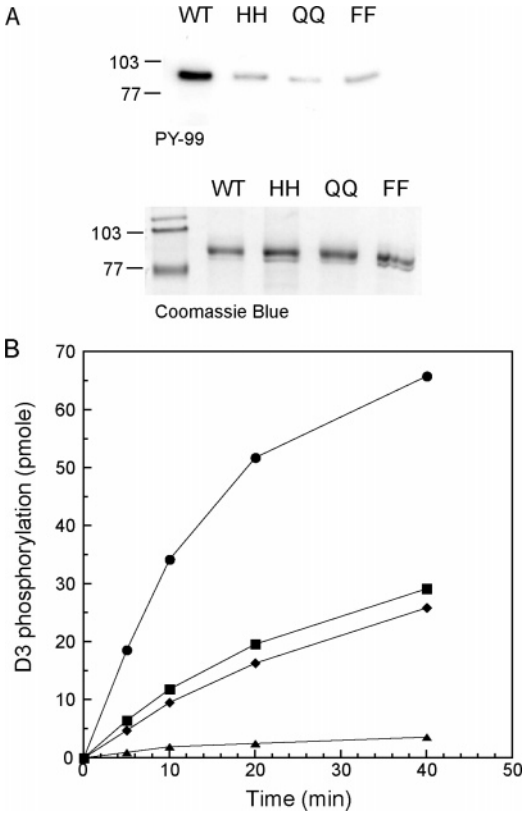


FIGURE 8: pY level (A) and in vitro activity (B) of the YXY domain mutants. (A) The pY level (top panel) was determined by immunoblotting 50 ng of each protein against antibody PY-99 as described above. Coomassie blue staining (bottom panel) of 0.5 μg of each protein was used as the loading control. (B) Time course D3 phosphorylation was performed similarly as described in the legend of Figure 3. The data represent the average of three trials: (●) WT, (■) HH, (◆) QQ, and (▲) FF.

the same as that of WT GST-497; neither requires pY for enzymatic activity.

DYRK1A has been suggested to form oligomers (*45*). If tyrosine phosphorylation is required for proper formation of the tertiary structure and for subsequent kinase activity, this requirement may be masked in GST fusion proteins. Therefore, full-length DYRK1A without GST fusion was subsequently prepared and subjected to the same analysis. Again, *E. coli*-expressed protein was found to contain pY, and its activity in phosphorylating D3 was not altered when pY was removed by LAR treatment (data not shown).

*Activity of DYRK1A Harboring YXY Motif Mutations*. Although phenylalanine and tyrosine are structurally similar, phenylalanine may not be a suitable substitution for addressing the role of tyrosine phosphorylation because it does not form hydrogen bonds and it is more likely to be buried inside a protein than tyrosine (*46*). Thus, the lack of function caused by conformational alterations may be misinterpreted as being caused by the loss of the hydroxyl group. Therefore, two additional YXY motif mutants with a hydrophilic substitution, histidine (HH) and glutamine (QQ), at both Y319 and Y321 were constructed on the truncated DYRK1A for analysis. Replacing the tyrosine residues with either histidine, glutamine, or phenylalanine caused a reduction in the level of pY (Figure 8A). These proteins were then subjected to the kinase assay using D3 as the substrate. Like that of the full-length protein, the enzymatic activity of WT GST-497 was largely eliminated by Y319F and Y321F double

Table 3: Kinetic Parameters (mean ± standard deviation) D3 Phosphorylation[a] of YXY Motif Mutants

| GST-497 | apparent $K_m$ ($\mu$M) | apparent $k_{cat}$ (min$^{-1}$) |
|---|---|---|
| WT | 43.63 ± 9.59 | 14.20 ± 2.43 |
| HH | 61.48 ± 18.27 | 4.55 ± 1.08 |
| QQ | 67.32 ± 12.86 | 3.26 ± 0.65 |
| FF | ND[b] | ND[b] |

[a] Performed with a constant ATP concentration of 50 $\mu$M. [b] Not determined due to low activity.

substitution (FF) (Figure 8B). On the other hand, despite lacking tyrosine residues in the YXY motif, both HH and QQ still retained a significant fraction (≥20−30%) of DYRK1A activity (Figure 8B and Table 3).

Subsequently, we used the Gli 1-dependent transcription, whose activity depends on DYRK1A (*47*), to measure the activity of these YXY motif mutants in cultured cells. To facilitate the assay, all YXY motif mutants were first reconstructed from the truncated mutants to the full-length clone in the pcDNA3 mammalian expression vector. Experiments were performed by transiently transfecting COS 7 cells with a mixture of the Gli 1 expression vector (*35*) and a luciferase reporter vector containing the Gli 1 binding sequence (*48*). As expected, the inclusion of the WT DYRK1A vector in the cotransfection consistently improved the luciferase output by ~6−7-fold under our assay conditions (Figure 9A). Under the same conditions, mutant FF was found to display ~4% of the WT activity (Figure 9A). However, mutants HH (~23% of that of WT) and QQ (~15% of that of WT) were significantly more active than mutant FF (Figure 9A), despite the fact that none of them contain a tyrosine residue in the YXY motif. The activity of the YXY mutants in vivo parallels that in vitro; both observations suggest that tyrosine residues in the YXY motif are not an absolute requirement for the activity of DYRK1A. WT and all YXY mutants were expressed at comparable levels in COS7 cells (Figure 9B), ruling out the protein expression level as a contributing factor to the difference in promoting the Gli 1-dependent transcription in vivo.

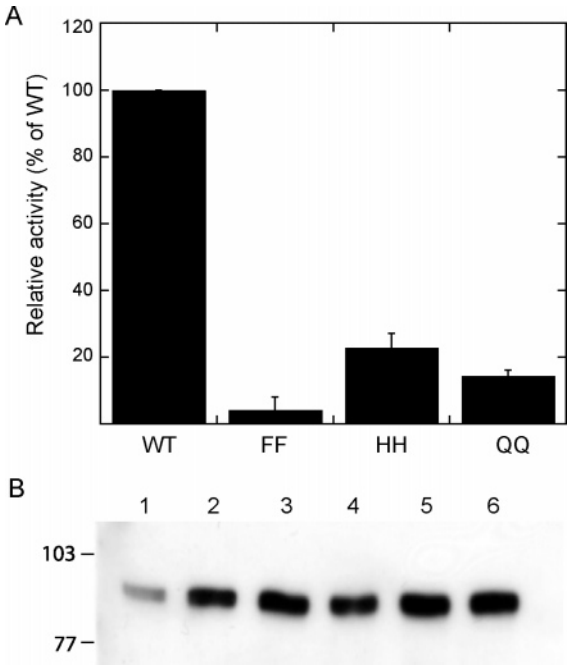


FIGURE 9: Activity (A) and level of expression (B) of YXY domain mutants in COS7 cells. The YXY domain mutants were first restored to the full-length clones in the pcDNA3 vector and then used to promote the Gli 1-dependent transcription in COS7 cells using luciferase as the reporter. The luciferase output was first corrected for the background (activity promoted by pcDNA3) and then normalized to the WT (100%) before being plotted. The data represent the average from three independent trials. The level of total DYRK1A in the lysate (used for the luciferase assay) was detected by immunoblotting using antibody 7F3. Cells were cotransfected with 0.1 $\mu$g of pcDNA3 (lane 1), 0.1 $\mu$g of pcMNB-(WT) (lane 2), 0.2 $\mu$g of pcMNB(WT) (lane 3), 0.2 $\mu$g of pcMNB-(FF) (lane 4), 0.2 $\mu$g of pcMNB(HH) (lane 5), or 0.2 $\mu$g of pcMNB(QQ) (lane 6).

## DISCUSSION

The YXY motif is conserved among members of the DYRK family (*3*). It has been hypothesized that the motif is the structural equivalent of the activation loop of MAPK (*18*, *19*) and that phosphorylation at the motif is required for DYRK1A activation (*1*, *19*). The hypothesis was directly examined in this study.

DYRK1A lacking detectable levels of pY by immunoblotting was prepared by LAR hydrolysis (Figure 1). When pY-dep DYRK1A was incubated under the conditions routinely employed for measuring DYRK1A activity, no detectable pY was regenerated after incubation for 20−30 min (Figure 2). Despite lacking pY, pY-dep DYRK1A was found to be equally active as the pY-containing untreated DYRK1A in autophosphorylation (Figure 4) and phosphorylation of various exogenous substrates in vitro (Figures 5 and S4). Similar to LAR, phosphatase $\lambda$PPase was also found to hydrolyze pY321 efficiently from WT GST-497 (Figure 6A and Table 2) without affecting the catalytic activity of WT GST-497 (Figure 6B). However, our results also demonstrate that the data obtained with $\lambda$PPase-treated samples must be interpreted cautiously because of the broad phosphatase activity of $\lambda$PPase, which may hydrolyze the very phosphorylated substrate used for monitoring the progress of the reaction (Figure S2). The use of $\lambda$PPase is further complicated by the fact that a simple method, such as glutathione affinity chromatography, is not sufficient to remove all $\lambda$PPase from the treated sample (data not shown).

Some may argue that the reason for not detecting a change in activity after phosphatase hydrolysis is due to very low stoichiometry of Y321 phosphorylation in *E. coli*-expressed DYRK1A. Apparently, this is not the case as the *E. coli*-expressed WT GST-497 appears to contain a substantial level of pY321 (Figure 7 and Table 2). The stoichiometry of Y321 phosphorylation was estimated to be at least 40% by assuming that the phosphorylated and nonphosphorylated YQY peptides have the same ionization efficiency. If anything, the stoichiometry of the phosphorylated peptide may be underestimated as the phosphorylated peptides are generally ionized less efficiently than the unphosphorylated counterpart in positive ion MS mode (*49*). However, even if the stoichiometry of Y321 phosphorylation is low, the activity change upon dephosphorylation could still be detectable as long as phosphorylation activates DYRK1A by a significant margin. MS analysis further confirmed that either LAR or $\lambda$PPase could readily remove pY321 from WT GST-497, especially for $\lambda$PPase, which removes nearly all pY321 (Table 2). The substantial reduction in the level of pY321 was clearly not accompanied with by corresponding reduction

in kinase activity. Our results support the conclusion that Y321 phosphorylation is not required for DYRK1A activity. Y111 is highly phosphorylated in *E. coli*-expressed DYRK1A, and the phosphorylation can be quantitatively removed by phosphatase treatment (data not shown). Phosphorylation and dephosphorylation at this residue may account for most of the changes observed in the anti-pY antibody staining.

We subsequently investigated whether tyrosine residues of the YXY motif were dispensable by replacing these residues with either histidine or glutamate. Similar to that of the FF mutant, the pY level is reduced in both the HH and QQ mutants (Figure 8). However, in contrast to the FF mutant, which contains little kinase activity, both the HH and QQ mutants retained significant levels of enzymatic activity in vitro (Figure 8B and Table 3). Furthermore, by using the Gli 1-dependent transcription system for assessing the activity of DYRK1A in cultured cells (Figure 9), we have also found that both the HH and QQ mutants are appreciably more active than the FF mutant in COS7 cells. Nevertheless, both the HH and QQ mutants still suffer from significant activity reduction when compared to that of WT. This indicates that the region at or near the YXY motif is important for kinase activity and that neither histidine nor glutamine is an optimal substitution for maintaining proper local protein structures. This is in agreement with the finding that the region immediately following the YXY motif is highly conserved for the DYRK family (*3*, *50*) and specifically the Q323 residue is important for the DYRK1A activity (*51*). However, the fact that the YXY motif tolerates substitutions suggests that tyrosine residues (and phosphorylation) in the YXY motif do not play a direct role in regulating the activity of DYRK1A. The results also support speculation that the lack of enzymatic activity associated with the FF mutant is more likely to be a result of a conformational alteration in or near the YXY motif rather than a result of the loss of the phosphorylatable residues at positions 319 and 321. The hydroxyl group of the tyrosine residue could serve as the recipient of a hydrogen bond, which may be required for stabilization of the region around the YXY motif. Furthermore, according to the model developed by Chothia (*46*), the FF substitutions would have drastically increased the hydrophobicity around the YXY motif and enhanced the probability of the YXY motif being buried inside the polypeptide. In contrast, little change in surface accessibility is predicated for the HH and QQ mutants. This reduced surface accessibility may further augment the consequences of the loss of hydrogen bonding in the FF mutant.

The reason for the inability of the pY-depleted but enzymatically active DYRK1A to regenerate pY can be satisfactorily addressed by inferring from the study delineating the mechanism of autophosphorylation in dDYRK2 and *Drosophila* MNB (*34*). Similar to DYRK1A, both mature dDYRK2 and *Drosophila* MNB are unable to produce pY via autophosphorylation. Instead, these kinases appear to acquire pY during certain intermediate steps of translation by means of intramolecular autophosphorylation (*34*). Since all these proteins are highly conserved, it is likely that DYRK1A is also utilizing the same mechanism to produce pY. That explains the inability of pY-dep DYRK1A to recuperate pY during autophosphorylation. The mechanism was further proposed to be the one-off inceptive event for the activation of dDYRK2, *Drosophila* MNB, and possibly other related kinases (*34*). If this is indeed the case for DYRK1A, the involvement of pY must be limited only to the processes prior to protein maturation, as the removal of pY has little effect on the kinetic activity of the mature kinase.

The physiological significance of Y321 phosphorylation is not clear since the enzymatic activity and tyrosine phosphorylation are apparently not directly related. It is possible that Y321 phosphorylation is a mere opportunistic byproduct of DYRK1A kinase activity or that it may have other functions that have yet to be defined. Tyrosine phosphorylation is apparently involved in maintaining the tertiary structure of MIRK/DYRK1B, a close relative of DYRK1A (*52*). In addition, proteins containing the SH2 domain are known to interact with pY (*53*). These protein−protein interactions may be crucial for the proper functioning, such as further activation or localization, of DYRK1A in vivo. Regardless, it is clear that the presence of pY should not be used as the sole index for DYRK1A activation. A direct kinase assay should be employed whenever possible (*11*, *31*−*33*).

Many members of the DYRK family were shown to contain pY in the YXY motif (*3*, *5*, *6*, *19*, *31*, *33*). Our finding that tyrosine phosphorylation is not essential for the activity of DYRK1A may not be applicable to every member of the family. For example, protein tyrosine phosphatase treatment was found to reduce the kinase activity along with the pY content in *S. cerevisiae* Yak1p (*31*), dDYRK2, and *Drosophila* MNB (*33*, *34*). Those results directly contrast our findings for phosphatase-treated DYRK1A. However, those studies used immunoprecipitated proteins instead of purified proteins for analysis. The contribution of kinase-associated factors to the activity of the kinase cannot be assessed in those cases. Furthermore, the activity of Pom1p from fission yeast is abolished when Y857 and Y859 (corresponding to Y319 and Y321, respectively, of DYRK1A) are substituted with aspartate (*11*), while DYRK3 appears to retain most of its activity when the corresponding tyrosine residues, Y331 and Y333, are replaced with glutamate (*32*). Those studies suggest that despite sharing numerous sequence homologies, different members of the DYRK family may employ different mechanisms for regulating the kinase activity. A generalized scheme cannot be drawn at present until more examples are examined. The mode of DYRK1A activation is clearly different from that of MAPK, which is turned on by activation lip phosphorylation (*20*). Many kinases are regulated through interactions with other factors. DYRK1A may belong to this class of kinases. In fact, protein 14-3-3 was shown to bind and promote DYRK1A activity (*54*, *55*). The interactions between DYRK1A and protein 14-3-3 appear to be regulated by DYRK1A phosphorylation at S520 (*55*). Whether this represents the mechanism for regulating cellular DYRK1A activity has yet to be elucidated.

## ACKNOWLEDGMENT

We thank Drs. Robert Denman, Robert Gould, and David Miller for critical reading of the manuscript.

## SUPPORTING INFORMATION AVAILABLE

Four supplemental figures (S1−S4). This material is available free of charge via the Internet at http://pubs.acs.org.

## REFERENCES


1. Kentrup, H., Becker, W., Heukelbach, J., Wilmes, A., Schürmann, A., Huppertz, C., Kainulainen, H., and Joost, H. G. (1996) Dyrk, a dual specificity protein kinase with unique structural features whose activity is dependent on tyrosine residues between subdomains VII and VIII, *J. Biol. Chem. 271*, 3488−3495.
2. Tejedor, F., Zhu, X. R., Kaltenbach, E., Ackermann, A., Baumann, A., Canal, I., Heisenberg, M., Fischbach, K. F., and Pongs, O. (1995) minibrain: A new protein kinase family involved in postembryonic neurogenesis in *Drosophila*, *Neuron 14*, 287−301.
3. Becker, W., and Joost, H. G. (1999) Structural and functional characteristics of Dyrk, a novel subfamily of protein kinases with dual specificity, *Prog. Nucleic Acid Res. Mol. Biol. 62*, 1−17.
4. Garrett, S., and Broach, J. R. (1989) Loss of Ras activity in *Saccharomyces cerevisiae* is suppressed by disruptions of a new kinase gene, YAK1, whose product may act downstream of the cAMP-dependent protein kinase, *Genes Dev. 3*, 1336−1348.
5. Becker, W., Weber, Y., Wetzel, K., Eirmbter, K., Tejedor, F. J., and Joost, H. G. (1998) Sequence characteristics, subcellular localization, and substrate specificity of DYRK-related kinases, a novel family of dual specificity protein kinases, *J. Biol. Chem. 273*, 25893−25902.
6. Lee, K., Deng, X., and Friedman, E. (2000) Mirk protein kinase is a mitogen-activated protein kinase substrate that mediates survival of colon cancer cells, *Cancer Res. 60*, 3631−3637.
7. Hämmerle, B., Carnicero, A., Elizalde, C., Ceron, J., Martínez, S., and Tejedor, F. J. (2003) Expression patterns and subcellular localization of the Down syndrome candidate protein MNB/DYRK1A suggest a role in late neuronal differentiation, *Eur. J. Neurosci. 17*, 2277−2286.
8. Moilanen, A. M., Karvonen, U., Poukka, H., Janne, O. A., and Palvimo, J. J. (1998) Activation of Androgen Receptor Function by a Novel Nuclear Protein Kinase, *Mol. Biol. Cell 9*, 2527−2543.
9. Hofmann, T. G., Mincheva, A., Lichter, P., Droge, W., and Schmitz, M. L. (2000) Human homeodomain-interacting protein kinase-2 (HIPK2) is a member of the DYRK family of protein kinases and maps to chromosome 7q32-q34, *Biochimie 82*, 1123−1127.
10. Shang, E., Wang, X., Huang, J., Yoshida, W., Kuroiwa, A., and Wolgemuth, D. J. (2000) Murine Myak, a member of a family of yeast YAK1-related genes, is highly expressed in hormonally modulated epithelia in the reproductive system and in the embryonic central nervous system, *Mol. Reprod. Dev. 55*, 372−378.
11. Bahler, J., and Nurse, P. (2001) Fission yeast Pom1p kinase activity is cell cycle regulated and essential for cellular symmetry during growth and division, *EMBO J. 20*, 1064−1073.
12. Shindoh, N., Kudoh, J., Maeda, H., Yamaki, A., Minoshima, S., Shimizu, Y., and Shimizu, N. (1996) Cloning of a human homolog of the *Drosophila* minibrain/rat DyrK gene from "the Down syndrome critical region" of chromosome 21, *Biochem. Biophys. Res. Commun. 225*, 92−99.
13. Guimerá, J., Casas, C., Pucharcòs, C., Solans, A., Domènech, A., Planas, A. M., Ashley, J., Lovett, M., Estivill, X., and Pritchard, M. A. (1996) A human homologue of *Drosophila* minibrain (MNB) is expressed in the neuronal regions affected in Down syndrome and maps to the critical region, *Hum. Mol. Genet. 5*, 1305−1310.
14. Song, W. J., Sternberg, L. R., Kasten-Sportès, C., Van Keuren, M. L., Chung, S. H., Slack, A., Miller, D. E., Glover, T. W., Chiang, P. W., Lou, L., and Kurnit, D. M. (1996) Isolation of human and murine homologues of the *Drosophila* minibrain gene: Human homologue maps to 21q22.2 in the Down syndrome "critical region", *Genomics 38*, 331−339.
15. Hammerle, B., Elizalde, C., Galceran, J., Becker, W., and Tejedor, F. J. (2003) The MNB/DYRK1A protein kinase: Neurobiological functions and Down syndrome implications, *J. Neural Transm., Suppl.*, 129−137.
16. Galceran, J., de Graaf, K., Tejedor, F. J., and Becker, W. (2003) The MNB/DYRK1A protein kinase: Genetic and biochemical properties, *J. Neural Transm., Suppl.*, 139−148.
17. Hanks, S. K., Quinn, A. M., and Hunter, T. (1988) The protein kinase family: Conserved features and deduced phylogeny of the catalytic domains, *Science 241*, 42−52.
18. Miyata, Y., and Nishida, E. (1999) Distantly related cousins of MAP kinase: Biochemical properties and possible physiological functions, *Biochem. Biophys. Res. Commun. 266*, 291−295.
19. Himpel, S., Panzer, P., Eirmbter, K., Czajkowska, H., Sayed, M., Packman, L. C., Blundell, T., Kentrup, H., Grotzinger, J., Joost, H. G., and Becker, W. (2001) Identification of the autophosphorylation sites and characterization of their effects in the protein kinase DYRK1A, *Biochem. J. 359*, 497−505.
20. Cobb, M. H., and Goldsmith, E. J. (1995) How MAP kinases are regulated, *J. Biol. Chem. 270*, 14843−14846.
21. Himpel, S., Tegge, W., Frank, R., Leder, S., Joost, H. G., and Becker, W. (2000) Specificity determinants of substrate recognition by the protein kinase DYRK1A, *J. Biol. Chem. 275*, 2431−2438.
22. Woods, Y. L., Cohen, P., Becker, W., Jakes, R., Goedert, M., Wang, X., and Proud, C. G. (2001) The kinase DYRK phosphorylates protein-synthesis initiation factor eIF2B$\epsilon$ at Ser539 and the microtubule-associated protein tau at Thr212: Potential role for DYRK as a glycogen synthase kinase 3-priming kinase, *Biochem. J. 355*, 609−615.
23. Woods, Y. L., Rena, G., Morrice, N., Barthel, A., Becker, W., Guo, S., Unterman, T. G., and Cohen, P. (2001) The kinase DYRK1A phosphorylates the transcription factor FKHR at Ser329 in vitro, a novel in vivo phosphorylation site, *Biochem. J. 355*, 597−607.
24. Matsuo, R., Ochiai, W., Nakashima, K., and Taga, T. (2001) A new expression cloning strategy for isolation of substrate-specific kinases by using phosphorylation site-specific antibody, *J. Immunol. Methods 247*, 141−151.
25. Campbell, L. E., and Proud, C. G. (2002) Differing substrate specificities of members of the DYRK family of arginine-directed protein kinases, *FEBS Lett. 510*, 31−36.
26. Skurat, A. V., and Dietrich, A. D. (2004) Phosphorylation of Ser640 in muscle glycogen synthase by DYRK family protein kinases, *J. Biol. Chem. 279*, 2490−2498.
27. Huang, Y., Chen-Hwang, M. C., Dolios, G., Murakami, N., Padovan, J., Wang, R., and Hwang, Y. W. (2004) Mnbk/Dyrk1A Phosphorylation Regulates the Interaction of Dynamin 1with SH3 Domain-Containing Proteins, *Biochemistry 43*, 10173−10185.
28. de Graaf, K., Hekerman, P., Spelten, O., Herrmann, A., Packman, L. C., Bussow, K., Muller-Newen, G., and Becker, W. (2004) Characterization of cyclin L2, a novel cyclin with an arginine/serine-rich domain: Phosphorylation by DYRK1A and colocalization with splicing factors, *J. Biol. Chem. 279*, 4612−4624.
29. de Graaf, K., Czajkowska, H., Rottmann, S., Packman, L. C., Lilischkis, R., Luscher, B., and Becker, W. (2006) The protein kinase DYRK1A phosphorylates the splicing factor SF3b1/SAP155 at Thr434, a novel in vivo phosphorylation site, *BMC Biochem. 7*, 7.
30. Murakami, N., Xie, W., Lu, R. C., Chen-Hwang, M. C., Wieraszko, A., and Hwang, Y. W. (2006) Phosphorylation of amphiphysin 1 by Mnb/Dyrk1A, a kinase implicated in Down syndrome, *J. Biol. Chem. 281*, 23712−23724.
31. Kassis, S., Melhuish, T., Annan, R. S., Chen, S. L., Lee, J. C., Livi, G. P., and Creasy, C. L. (2000) *Saccharomyces cerevisiae* Yak1p protein kinase autophosphorylates on tyrosine residues and phosphorylates myelin basic protein on a C-terminal serine residue, *Biochem. J. 348*, 263−272.
32. Li, K., Zhao, S., Karur, V., and Wojchowski, D. M. (2002) DYRK3 activation, engagement of protein kinase A/cAMP response element-binding protein, and modulation of progenitor cell survival, *J. Biol. Chem. 277*, 47052−47060.
33. Lochhead, P. A., Sibbet, G., Kinstrie, R., Cleghon, T., Rylatt, M., Morrison, D. K., and Cleghon, V. (2003) dDYRK2: A novel dual-specificity tyrosine-phosphorylation-regulated kinase in *Drosophila*, *Biochem. J. 374*, 381−391.
34. Lochhead, P. A., Sibbet, G., Morrice, N., and Cleghon, V. (2005) Activation-Loop Autophosphorylation Is Mediated by a Novel Transitional Intermediate Form of DYRKs, *Cell 121*, 925−936.
35. Kinzler, K. W., Ruppert, J. M., Bigner, S. H., and Vogelstein, B. (1988) The GLI gene is a member of the Kruppel family of zinc finger proteins, *Nature 332*, 371−374.
36. Chen-Hwang, M. C., Chen, H. R., Elzinga, M., and Hwang, Y. W. (2002) Dynamin is a minibrain kinase/dual specificity Yak1-related kinase 1A substrate, *J. Biol. Chem. 277*, 17597−17604.
37. Adayev, T., Chen-Hwang, M. C., Murakami, N., Wegiel, J., and Hwang, Y. W. (2006) Kinetic property of a MNB/DYRK1A mutant suitable for the elucidation of biochemical pathways, *Biochemistry 45*, 12011−12019.
38. Hwang, Y. W., Zhong, J. M., Poullet, P., and Parmeggiani, A. (1993) Inhibition of SDC25 C-domain-induced guanine-nucleotide

exchange by guanine ring binding domain mutants of v-H-*ras*, *J. Biol. Chem. 268*, 24692−24698.
39. Sung, Y. J., Carter, M., Zhong, J. M., and Hwang, Y. W. (1995) Mutagenesis of the H-ras p21 at glycine-60 residue disrupts GTP-induced conformational change, *Biochemistry 34*, 3470−3477.
40. Wegiel, J., Kuchna, I., Nowicki, K., Frackowiak, J., Dowjat, K., Silverman, W. P., Reisberg, B., DeLeon, M., Wisniewski, T., Adayev, T., Chen-Hwang, M. C., and Hwang, Y. W. (2004) Cell type- and brain structure-specific patterns of distribution of minibrain kinase in human brain, *Brain Res. 1010*, 69−80.
41. Hunter, T., and Sefton, B. M. (1980) Transforming gene product of Rous sarcoma virus phosphorylates tyrosine, *Proc. Natl. Acad. Sci. U.S.A. 77*, 1311−1315.
42. Shevchenko, A., Wilm, M., Vorm, O., and Mann, M. (1996) Mass spectrometric sequencing of proteins silver-stained polyacrylamide gels, *Anal. Chem. 68*, 850−858.
43. Cohen, P. T., and Cohen, P. (1989) Discovery of a protein phosphatase activity encoded in the genome of bacteriophage *λ*. Probable identity with open reading frame 221, *Biochem. J. 260*, 931−934.
44. Zhuo, S., Clemens, J. C., Hakes, D. J., Barford, D., and Dixon, J. E. (1993) Expression, purification, crystallization, and biochemical characterization of a recombinant protein phosphatase, *J. Biol. Chem. 268*, 17754−17761.
45. Song, W. J., Chung, S. H., and Kurnit, D. M. (1997) The murine Dyrk protein maps to chromosome 16, localizes to the nucleus, and can form multimers, *Biochem. Biophys. Res. Commun. 231*, 640−644.
46. Chothia, C. (1976) The nature of the accessible and buried surfaces in proteins, *J. Mol. Biol. 105*, 1−12.
47. Mao, J., Maye, P., Kogerman, P., Tejedor, F. J., Toftgard, R., Xie, W., Wu, G., and Wu, D. (2002) Regulation of Gli1 Transcriptional Activity in the Nucleus by Dyrk1, *J. Biol. Chem. 277*, 35156−35161.
48. Sasaki, H., Hui, C., Nakafuku, M., and Kondoh, H. (1997) A binding site for Gli proteins is essential for HNF-3*β* floor plate enhancer activity in transgenics and can respond to Shh in vitro, *Development 124*, 1313−1322.
49. Simpson, R. J. (2002) *Proteins and Proteomics: A Laboratory Manual*, Cold Spring Harbor Laboratory Press, Plainview, NY.
50. Kannan, N., and Neuwald, A. F. (2004) Evolutionary constraints associated with functional specificity of the CMGC protein kinases MAPK, CDK, GSK, SRPK, DYRK, and CK2α, *Protein Sci. 13*, 2059−2077.
51. Wiechmann, S., Czajkowska, H., de Graaf, K., Grotzinger, J., Joost, H. G., and Becker, W. (2003) Unusual function of the activation loop in the protein kinase DYRK1A, *Biochem. Biophys. Res. Commun. 302*, 403−408.
52. Zou, Y., Lim, S., Lee, K., Deng, X., and Friedman, E. (2003) Serine/threonine kinase Mirk/Dyrk1B is an inhibitor of epithelial cell migration and is negatively regulated by the Met adaptor Ran-binding protein M, *J. Biol. Chem. 278*, 49573−49581.
53. Schlessinger, J. (1994) SH2/SH3 signaling proteins, *Curr. Opin. Genet. Dev. 4*, 25−30.
54. Kim, D., Won, J., Shin, D. W., Kang, J., Kim, Y. J., Choi, S. Y., Hwang, M. K., Jeong, B. W., Kim, G. S., Joe, C. O., Chung, S. H., and Song, W. J. (2004) Regulation of Dyrk1A kinase activity by 14-3-3, *Biochem. Biophys. Res. Commun. 323*, 499−504.
55. Alvarez, M., Altafaj, X., Aranda, S., and de la Luna, S. (2007) DYRK1A Autophosphorylation on Serine Residue 520 Modulates Its Kinase Activity via 14-3-3 Binding, *Mol. Biol. Cell 18*, 1167−1178.

BI700251N